Scientia Iranica, Vol. 13, No. 2, pp 113–123

SCIENTIA IRANICA

Buckling of Discretely Stringer-Stiffened Composite Cylindrical Shells under Combined Axial Compression and External Pressure

D. Poorveis[1] and M.Z. Kabir*

In this paper, the static buckling of especially orthotropic stringer-stiffened composite cylindrical shells subjected to combined axial compression and external pressure is investigated, based on geometrical non-linear analysis with considering pre-buckling deformations. The kinematic relation of shells is based on the Donnell non-linear theory and First Order Shear Deformation (FOSD) is adopted for both shell and stiffeners. Displacements, rotations and interacting forces are expressed in terms of Fourier series expansions as independent approximate solution functions. Unknown coefficients of shell and stringers are related by satisfying continuity conditions of displacements at their contact areas using Lagrange multipliers. The non-linear equilibrium equations are obtained using the Ritz method. The effects of sensitivity parameters, e.g., shell lay-ups, different numbers of stringers in the circumference, location of stiffeners (outside vs. inside) and the discrete versus smeared approach on interaction buckling curves are considered. Results indicate remarkable differences between outside and inside stringer-stiffened cylinder buckling loads and also illustrate the fundamental role of shell stacking sequences and stiffened shell geometry on the applicability range of the smeared stiffener approach.

INTRODUCTION

Stiffened thin cylindrical shells subject to combined external pressure and axial compression are widely used in aerospace structures and the offshore-oil industry. Research on the buckling and post-buckling of stringer-stiffened cylindrical shells in the past three decades have increased. In the context of experimental studies, various specimens with different shell and stringer geometry and boundary conditions were tested under axial compression by Weller and Singer [1]. Also, Singer and Abramovich [2] applied vibration tests to define practical boundary conditions in stiffened shells. Weller [3] studied the influence of in-plane boundary conditions on the critical load of axially compressed simply supported stringer-stiffened cylindrical shells. Sheinman, Shaw and Simitses [4] used a smeared stiffener technique for orthogonally stiffened laminated cylinders. Bushnell [5] developed PANDA, an interactive program, to design minimum weight stiffened cylindrical panel under combined in-plane loads. Discrete analysis of orthogonally stiffened composite cylindrical shells, subjected to combinations of uniform internal pressure, constant temperature changes and axial load, were investigated by Wang and Hsu [6]. Abramowitz, Weller and Singer [7] appraised the effect of a sequence of combined loading on the buckling of stiffened shells. They showed that order of loading does not affect the buckling loads. Ji and Yen [8] studied the buckling of orthogonally stiffened cylinders. They assumed that stringers can be closely spaced and treated by a smeared model but that part of a shell stiffened with rings was treated as a discrete shell element. A singular perturbation technique was used by Shen and his co-workers [9,10] to investigate the buckling and post-buckling behavior of perfect and imperfect stiffened cylinders. Dawe and Wang [11] applied a finite strip method to assess the post-buckling response of stiffened composite panels. The strip element with different nodal lines, was used for modeling

1. *Department of Civil and Environmental Engineering, Amirkabir University of Technology, Tehran, I.R. Iran.*
*. *Corresponding Author, Department of Civil and Environmental Engineering, Amirkabir University of Technology, Tehran, I.R. Iran.*

longitudinal stiffeners. The buckling of axially stiffened conical shells under axial compression was studied by Spagnoli [12]. Different modes of instability, in particular, local shell and stringer buckling modes and a global buckling mode through a linear eigenvalue finite element analysis were investigated. Haixu [13] derived equilibrium equations for a double cylindrical shell stiffened longitudinally and transversely and subjected to uniform hydrostatic external pressure by using an adjacent equilibrium method. He calculated the theoretically critical pressures of panel buckling and interframe shell buckling. The dynamic buckling of cylindrical stringer-stiffened shells was explored both numerically and experimentally by Yaffe and Abramovich [14]. They used the ADINA finite element code to simulate the static and dynamic buckling loads of the shells.

The current paper investigates the buckling of discretely stringer-stiffened laminated cylindrical shells subject to combined external pressure and axial compression. The boundary conditions are assumed to be classical and simply supported. Initial imperfection is in the form of a buckling mode and its amplitude is taken as small so as not to affect the buckling load. The critical load is calculated by controlling the determinant sign of the tangent stiffness matrix. Various stringer-stiffened composite cylinders, differing in the number of stiffeners, laminate architectures and location of stringer (outside vs. inside), are analyzed to estimate the range of applicability of the smeared stiffener model. Interaction buckling curves are plotted for different cases and, to compare the results, more concentration is put on these curves.

THEORY

For the discrete model, displacements, rotations and interaction forces are expressed in terms of Fourier series expansions as independent approximate solution functions. These functions are related by continuity conditions of displacement between the shell and stiffeners at their contact area by Lagrange multiplier coefficients. The equilibrium equations are obtained using the Ritz method. The linearized equations can be solved using iterative Newton-Raphson and arc-length methods [15]. In the smeared stiffener approach, shell rigidities are modified based on material and geometrical properties and the spacing of stringers. Then, analysis, such as that of an unstiffened shell, is carried out.

SHELL AND STIFFENER GEOMETRY

The configuration of a shell with global coordinates is sketched in Figure 1. The principal material directions are specified as 1 and 2. The global coordinate system

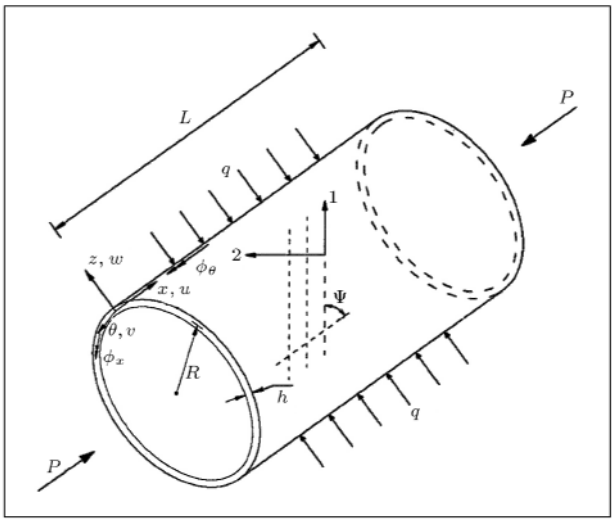

Figure 1. Cylindrical shell with coordinate system, key dimensions and loading.

x, θ and z, displacement components U, V, W and rotations ϕ_x and ϕ_θ are also shown in Figure 1. In the same figure, the lateral pressure, q, the axial force, P, the length, L, the thickness, h, and the radius of curvature of middle surface, R, are also shown. Ψ is the angle between the principal material axis, 1, and the x-axis of the shell. Also, deviation of the fiber direction in the stringer is measured, with respect to the longitudinal axis. Figure 2 shows the stringer coordinate axes x, θ and z in the longitudinal, circumferential and radial directions, respectively, which are located at its centroid and which are parallel to those of the shell. Displacements and rotations of the stiffener shown in the mentioned figure are also measured at the centroid. Interacting forces, as a result of the contact stresses, are depicted in this figure.

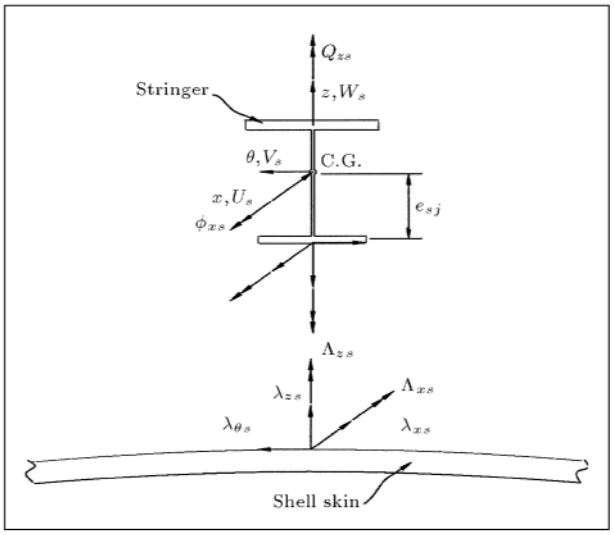

Figure 2. Stringer coordinate system and interacting forces between shell and stiffener.

DISPLACEMENTS AND ROTATIONS

The displacements of an arbitrary point of the cylindrical shell is expressed as:

$$\overline{U}(x,\theta,z) = U(x,\theta) + z\phi_x(x,\theta),$$

$$\overline{V}(x,\theta,z) = V(x,\theta) + z\phi_\theta(x,\theta),$$

$$\overline{W}(x,\theta,z) = W(x,\theta), \tag{1}$$

where $U(x,\theta)$, $V(x,\theta)$ and $W(x,\theta)$ are displacements of the mid-surface of the shell in axial, circumferential and radial directions, respectively, and $\phi_x(x,\theta)$ and $\phi_\theta(x,\theta)$ are the rotations of the normal vector to the surface. Similarly, the stringer displacements in x, θ and z directions are defined as [16]:

$$\overline{U}_s(x,\theta,z) = U_s(x) + z\phi_{\theta s}(x) \quad \mathrm{R}_0\theta\phi_{zs}(x) \quad \omega(\theta,z)\tau_s,$$

$$\overline{V}_s(x,z) = V_s(x) + z\phi_{xs},$$

$$\overline{W}_s(x,\theta) = W_s(x) \quad \mathrm{R}_0\theta\phi_{xs}, \tag{2}$$

where U_s, V_s and W_s are stiffener centroid displacements and ϕ_{xs}, $\phi_{\theta s}$ and ϕ_{zs} are rotations of the stiffener about the mentioned axes, respectively. $\omega(\theta,z)$ is a warping function of the stiffener cross section, R_0 is the distance between the stringer centroid and the center of the cylinder and τ_s is the unknown warping coefficient. Neglecting the shear strain in warping, τ_s becomes:

$$\tau_s = \frac{\partial\phi_{xs}}{\partial x}. \tag{3}$$

STRAIN-DISPLACEMENT RELATIONSHIPS

The strain-displacement relationships at an arbitrary point of the shell thickness can be expressed as follows:

$$e_x = \varepsilon_x + z\kappa_x, \quad e_\theta = \varepsilon_\theta + z\kappa_\theta, \quad e_{x\theta} = \gamma_{x\theta} + z\kappa_{x\theta}, \tag{4}$$

where strains of mid-plane and curvatures, based on Donnell and the first order shear deformation theories and initial imperfection ($\hat{W}$), are as follows:

$$\varepsilon_x = \frac{\partial U}{\partial x} + \frac{1}{2}\left(\frac{\partial W}{\partial x}\right)^2 + \left(\frac{\partial \hat{W}}{\partial x}\right)\left(\frac{\partial W}{\partial x}\right),$$

$$\varepsilon_\theta = \frac{1}{\mathrm{R}}\frac{\partial V}{\partial\theta} + \frac{W}{R} + \frac{1}{2\mathrm{R}^2}\left(\frac{\partial W}{\partial\theta}\right)^2 + \frac{1}{\mathrm{R}^2}\left(\frac{\partial \hat{W}}{\partial\theta}\right)\left(\frac{\partial W}{\partial\theta}\right),$$

$$\gamma_{x\theta} = \frac{1}{\mathrm{R}}\frac{\partial U}{\partial\theta} + \frac{\partial V}{\partial x} + \frac{1}{\mathrm{R}}\left(\frac{\partial W}{\partial x}\right)\left(\frac{\partial W}{\partial\theta}\right) + \frac{1}{\mathrm{R}}\left(\frac{\partial W}{\partial x}\right)\left(\frac{\partial \hat{W}}{\partial\theta}\right) + \frac{1}{\mathrm{R}}\left(\frac{\partial \hat{W}}{\partial x}\right)\left(\frac{\partial W}{\partial\theta}\right),$$

$$\kappa_x = \frac{\partial\phi_x}{\partial x}, \quad \kappa_\theta = \frac{1}{\mathrm{R}}\frac{\partial\phi_\theta}{\partial\theta}, \quad \kappa_{x\theta} = \frac{1}{\mathrm{R}}\frac{\partial\phi_x}{\partial\theta} + \frac{\partial\phi_\theta}{\partial x},$$

$$\gamma_{xz} = \phi_x + \frac{\partial W}{\partial x}, \quad \gamma_{\theta z} = \phi_\theta + \frac{1}{\mathrm{R}}\left(\frac{\partial W}{\partial\theta}\right). \tag{5}$$

Similarly, for stringer, the non-zero strains are:

$$e^s_{xx} = \frac{\partial\overline{U}_s}{\partial x} + \frac{1}{2}\left(\frac{\partial W_s}{\partial x}\right)^2 + \frac{1}{2}\left(\frac{\partial V_s}{\partial x}\right)^2 + \left(\frac{\partial \hat{W}_s}{\partial x}\right)\left(\frac{\partial W_s}{\partial x}\right),$$

$$\gamma^s_{x\theta} = \frac{1}{\mathrm{R}_0}\frac{\partial\overline{U}_s}{\partial\theta} + \frac{\partial\overline{V}_s}{\partial x}, \quad \gamma^s_{xz} = \frac{\partial\overline{U}_z}{\partial z} + \frac{\partial\overline{W}_s}{\partial x}. \tag{6}$$

In these relations, $\hat{W}_s$ is the initial imperfection of the stringer, which is obtained by substitution of the stringer position ($\theta = \theta_s$) in the shell initial imperfection ($\hat{W}$). Due to the small rotations of stiffeners, only displacement components are retained in the nonlinear terms of strain. Using Equations 2, the strains are expressed in terms of displacements and rotations at the centroid.

CONSTITUTIVE EQUATIONS

The stress-strain relationship for the shell is expressed as:

$$\{\sigma\} = [C]\{\varepsilon\}, \tag{7}$$

where $[C]$ is the generalized material rigidity matrix. The vector of stress resultants is defined as:

$$\{\sigma\} = [N_x, N_\theta, N_{x\theta}, M_x, M_\theta, M_{x\theta}, Q_x, Q_\theta]^T, \tag{8}$$

N, M and Q are in-plane forces, moments and out of plane shear components in unit length, respectively. The generalized strain vector, $\{\varepsilon\}$, is:

$$\{\varepsilon\} = [\varepsilon_x, \varepsilon_\theta, \gamma_{x\theta}, \kappa_x, \kappa_\theta, \kappa_{x\theta}, \gamma_{xz}, \gamma_{\theta z}]^T, \tag{9}$$

where ε_x, ε_θ and $\gamma_{x\theta}$ are mid-surface strains and κ_x and κ_θ are bending curvatures in x z and θ z planes, respectively. $\kappa_{x\theta}$ is in-plane twist curvature andγ_{xz} and $\gamma_{\theta z}$ represent transverse shear strains. $[C]$ matrix is:

$$[C] = \begin{bmatrix} [A] & [B] & 0 & 0 \\ [B] & [D] & 0 & 0 \\ 0 & 0 & A_{44} & 0 \\ 0 & 0 & 0 & A_{55} \end{bmatrix}, \tag{10}$$

where A_{ij} are membrane rigidities, B_{ij} are membrane-bending coupling terms, D_{ij} are bending rigidities and transverse shear rigidities A_{44} and A_{55} are defined as:

$$(A_{ij}, B_{ij}, D_{ij}) = \int_h (1, z, z^2)\overline{Q}_{ij} dz,$$

$$A_{44} = \int_h \overline{Q}_{44} dz, \quad A_{55} = \int_h \overline{Q}_{55} dz, \tag{11}$$

where $\overline{Q}_{ij}$ is the transformed reduced stiffness [17]. The stress components corresponding to non-zero strains for the stiffener are σ^s_{xx}, $\sigma^s_{x\theta}$ and σ^s_{xz}. Stress-strain relations at a generic point in the stringer are expressed as:

$$\begin{Bmatrix} \sigma^s_{xx} \\ \sigma^s_{x\theta} \\ \sigma^s_{xz} \end{Bmatrix} = \begin{bmatrix} \overline{Q}^s_{11} & \overline{Q}^s_{16} & 0 \\ \overline{Q}^s_{16} & \overline{Q}^s_{66} & 0 \\ 0 & 0 & \overline{Q}^s_{44} \end{bmatrix} \begin{Bmatrix} e^s_{xx} \\ \gamma^s_{x\theta} \\ \gamma^s_{xz} \end{Bmatrix}, \tag{12}$$

where $\overline{Q}^s_{11}$, $\overline{Q}^s_{16}$, $\overline{Q}^s_{44}$ and $\overline{Q}^s_{66}$ are the transformed reduced stiffnesses for the stringer. In the case of orthotropic laminate, $\overline{Q}^s_{16}$ is zero. Integrating Equation 12 over the stiffener cross-section, the following constitutive equation is obtained.

$$\{N_{xs}, M_{\theta s}, M_{zs}, M_{\omega s}, T_{ss}, V_{\theta s}, V_{zs}\}^T =$$

$$[E_s]\{\varepsilon_{xs}, \kappa_{\theta s}, \kappa_{zs}, \kappa_{\omega s}, \gamma_{ss}, \gamma_{\theta s}, \gamma_{zs}\}^T, \tag{13}$$

where N_{xs}, $M_{\theta s}$, M_{zs}, $M_{\omega s}$ and T_{ss} are axial force, bending moments about axes θ and z, bimoment and uniform torsion, respectively. Also $V_{\theta s}$ and V_{zs} are shear forces in θ and z directions. The symmetric (7×7) matrix, $[E_s]$, is the elasticity tensor, which represents the material and geometrical properties of the stringer. Details of the deriving elements of $[E_s]$ for stiffener with an arbitrary thin-walled cross-section and with general orthotropic material can be found in [16,18]. The generalized strain vector, according to displacements and rotations of the stringer centroid, are:

$$\varepsilon_{xs} = \frac{\partial U_s}{\partial x} + \frac{1}{2}\left(\frac{\partial W_s}{\partial x}\right)^2 + \frac{1}{2}\left(\frac{\partial V_s}{\partial x}\right)^2 + \left(\frac{\partial \hat{W}_s}{\partial x}\right)\left(\frac{\partial W_s}{\partial x}\right),$$

$$\kappa_{\theta s} = \frac{\partial \phi_{\theta s}}{\partial x}, \quad \kappa_{zs} = \frac{\partial \phi_{zs}}{\partial x}, \quad \kappa_{\omega s} = \frac{\partial^2 \phi_{xs}}{\partial x^2},$$

$$\gamma_{ss} = \frac{\partial \phi_{xs}}{\partial x}, \quad \gamma_{\theta s} = \left(\frac{\partial V_s}{\partial x} \quad \phi_{zs}\right),$$

$$\gamma_{zs} = \left(\frac{\partial W_s}{\partial x} + \phi_{\theta s}\right), \tag{14}$$

where, ε_{xs} is the axial stretch, $\kappa_{\theta s}$, κ_{zs} and $\kappa_{\omega s}$ the bending and warping curvatures, respectively, and $\gamma_{\theta s}$ and γ_{zs} are transverse shear strains due to bending. Also, γ_{ss} represents the torsional curvature of the stringer.

FOURIER APPROXIMATIONS

For classical simply supported end conditions, the double expansions of the Fourier series for shell displacements and rotations are:

$$U(x,\theta) = (x \quad L/2)U_{x0} + \sum_{m=1}^{M}\sum_{n=0}^{N} U_{mn} \quad \cos(\alpha_m x) \quad \cos(n\theta),$$

$$V(x,\theta) = \sum_{m=1}^{M}\sum_{n=1}^{N} V_{mn} \quad \sin(\alpha_m x) \quad \sin(n\theta),$$

$$W(x,\theta) = \sum_{m=1}^{M}\sum_{n=0}^{N} W_{mn} \quad \sin(\alpha_m x) \quad \cos(n\theta),$$

$$\phi_x(x,\theta) = \sum_{m=1}^{M}\sum_{n=0}^{N} \phi_{xmn} \quad \cos(\alpha_m x) \quad \cos(n\theta),$$

$$\phi_\theta(x,\theta) = \sum_{m=1}^{M}\sum_{n=1}^{N} \phi_{\theta_{mn}} \quad \sin(\alpha_m x) \quad \sin(n\theta), \tag{15}$$

in which $\alpha_m = m\pi/L$ and M and N are the upper limit of integer numbers m and n. The unknown coefficients, U_{x0}, U_{mn}, V_{mn}, W_{mn}, ϕ_{xmn} and $\phi_{\theta mn}$, are obtained in each incremental step. The displacement and rotation functions of stiffeners are assumed as follows:

$$U_s(x) = (x \quad L/2)U_{s0} + \sum_{m=1}^{M} U_{sm}\cos(\alpha_m x),$$

$$V_s(x) = \sum_{m=1}^{M} V_{sm}\sin(\alpha_m x),$$

$$W_s(x) = \sum_{m=1}^{M} W_{sm}\sin(\alpha_m x),$$

$$\phi_{xs}(x) = \sum_{m=1}^{M} \phi_{xsm}\sin(\alpha_m x),$$

$$\phi_{\theta s}(x) = \sum_{m=0}^{M} \phi_{\theta sm}\cos(\alpha_m x),$$

$$\phi_{zs}(x) = \sum_{m=1}^{M} \phi_{zsm}\cos(\alpha_m x), \tag{16}$$

where U_{s0}, U_{sm}, V_{sm}, W_{sm}, ϕ_{xsm}, $\phi_{\theta sm}$ and ϕ_{zsm} are the stringer unknown coefficient. In Equations 15 and 16, U_{x0} and U_{s0} are required to ensure correct distribution of stresses in the shell and stringers for the pre-buckling state. The existing stresses at the interfacial area between cylindrical shell and stringer are shown in Figure 2, in terms of forces and moments per unit length, and their Fourier expansions are as follows:

$$\lambda_{xs}(x) = \sum_{m=1}^{M} \lambda_{xsm} \cos(\alpha_m x),$$

$$\lambda_{\theta s}(x) = \sum_{m=1}^{M} \lambda_{\theta sm} \sin(\alpha_m x),$$

$$\lambda_{zs}(x) = \sum_{m=1}^{M} \lambda_{zsm} \sin(\alpha_m x),$$

$$\Lambda_{xs}(x) = \sum_{m=1}^{M} \Lambda_{xsm} \sin(\alpha_m x),$$

$$\Lambda_{zs}(x) = \sum_{m=0}^{M} \Lambda_{zsm} \cos(\alpha_m x), \tag{17}$$

where λ_{xsm}, $\lambda_{\theta sm}$, λ_{zsm}, Λ_{xsm} and Λ_{zsm} are unknown coefficients. The continuity of displacements at the interface is required:

$$g_{xsj} = U(x,\theta_j) + \frac{h}{2}\phi_x(x,\theta_j)$$

$$[U_{sj}(x) + e_{sj}\phi_{\theta sj}(x) \quad \omega_{0j}\tau_{sj}(x)] = 0,$$

$$g_{\theta sj} = V(x,\theta_j) + \frac{h}{2}\phi_\theta(x,\theta_j)$$

$$[V_{sj}(x) + e_{sj}\phi_{xsj}(x)] = 0,$$

$$g_{zsj} = W(x,\theta_j) \quad W_{sj}(x) = 0,$$

$$G_{xsj} = \frac{\partial W}{\partial \theta}(x,\theta_j) + (R + h/2)\phi_{xsj}(x) = 0,$$

$$G_{zsj} = \frac{\partial U}{\partial \theta}(x,\theta_j) + \frac{h}{2}\frac{\partial \phi_x}{\partial \theta}(x,\theta_j)$$

$$+ [(R + h/2)\phi_{zsj}(x) + \omega_{1j}\tau_{sj}(x)] = 0. \tag{18}$$

The subscript, j, is related to the jth stringer and ω_{0j} and ω_{1j} are warping constants of the top flange, which is in contact with the shell. Also, e_{sj} is the distance from the centroid of the jth stringer to the contact surface. The variation limit of x is $0 \le x \le L$.

$$\omega_s(\theta, e_{sj}) = \omega_{0j} + \omega_{1j}\theta. \tag{19}$$

NON-LINEAR ANALYSIS (DISCRETE MODEL)

The equilibrium equations of stiffened cylinders are obtained by combining the internal virtual work of shells and stiffeners, external virtual work due to applied loads and the virtual work of interaction forces. The non-linear equations are solved by the Newton-Raphson method. The internal virtual work of the cylindrical shell is:

$$\delta W_{sh}^{\text{int}} = \iint_S \Big[N_x\delta\varepsilon_x + N_\theta\delta\varepsilon_\theta + N_{x\theta}\delta\gamma_{x\theta} + M_x\delta\kappa_x$$

$$+ M_\theta\delta\kappa_\theta + M_{x\theta}\delta\kappa_{x\theta} + Q_x\delta\gamma_{xz} + Q_\theta\delta\gamma_{\theta z}\Big]dS. \tag{20}$$

Also, the internal virtual work of longitudinal stiffeners is:

$$\delta W_s^{\text{int}} = \int_0^L [N_{xs}\delta\varepsilon_{xs} + M_{\theta s}\delta\kappa_{\theta s} + M_{zs}\delta\kappa_{zs} + M_{\omega s}\delta\kappa_{\omega s}$$

$$+ T_{ss}\delta\gamma_{ss} + V_{\theta s}\delta\gamma_{\theta s} + V_{zs}\delta\gamma_{zs}]dx. \tag{21}$$

The external virtual work, due to axial compression and external pressure, is:

$$\delta W_{sh}^{\text{ext}} = P\int_0^{2\pi} [\delta U(1,\theta) \quad \delta U(0,\theta)]Rd\theta \quad q^D\int_S \delta W\, dS. \tag{22}$$

In which P is the axial force per unit length of the cylinder circumference and q^D is the radial dead pressure. For hydrostatic pressure, P is related to $q^D (P = Rq^D/2)$. In the case of live external pressure, which is displacement dependent [19], the second term of Equation 22 is modified as:

$$q^L\int_S \left[\delta W + \frac{1}{R}(V\delta V + W\delta W) + \delta W\left(\frac{\partial U}{\partial x} + \frac{1}{R}\frac{\partial V}{\partial \theta}\right)\right.$$

$$\left. + W\left(\frac{\partial \delta U}{\partial x} + \frac{1}{R}\frac{\partial \delta V}{\partial \theta}\right)\right] dS. \tag{23}$$

The virtual work of interacting forces between shell and stiffeners, with respect to the continuity relations in Equations 18, is expressed as:

$$\delta W_\lambda = \sum_j \int_0^L \delta[\lambda_{xsj}g_{xsj} + \lambda_{zsj}g_{zsj} + \lambda_{\theta sj}g_{\theta sj}$$

$$+ \Lambda_{xsj}G_{xsj} + \Lambda_{zsj}G_{zsj}]dx. \tag{24}$$

In which $\sum_j$ exhibits summation over the total number of stringers. The total virtual work of the system is:

$$\delta W_{sh}^{\text{int}} + \delta W_{s}^{\text{int}} + \delta W_{\lambda} \quad \delta W_{sh}^{ext} = 0. \tag{25}$$

Linearization and discretization of Equation 25 leads to:

$$\begin{bmatrix} K_{sh}+K_L & 0 & K_{sh}^{\lambda s} \\ & K_s & K_{sh}^{\lambda s} \\ \text{Sym.} & & 0 \end{bmatrix} \begin{Bmatrix} \Delta\overline{U}_{sh} \\ \Delta\overline{U}_{s} \\ \Delta\overline{\lambda}_{s} \end{Bmatrix} = \begin{Bmatrix} \overline{R}_{sh} \\ \overline{R}_{s} \\ \overline{R}_{\lambda} \end{Bmatrix}$$

$$= \begin{Bmatrix} F_{sh}^{\text{ext}} & F_{sh}^{\text{int}} & F_{sh}^{\lambda s} \\ & F_{s}^{\text{int}} & F_{s}^{\lambda s} \\ & & F_{\lambda}^{\lambda s} \end{Bmatrix}. \tag{26}$$

In which K_{sh} and K_s are shell and stringer tangent stiffness matrices, respectively. K_L is the load stiffness matrix, which reflects live external pressure effects and $K_{sh}^{\lambda s}$ and $K_s^{\lambda s}$ are stiffness submatrices derived from interaction forces virtual work. Also, $\Delta\overline{U}_{sh}$ and $\Delta\overline{U}_s$ are shell and stiffener incremental displacement vectors and $\Delta\overline{\lambda}_s$ defines incremental interaction forces. Residual forces obtained from Equations 20 to 25 are in the right hand side of Equation 26. To solve Equation 26, non-linear in shell and stiffener displacements, the coefficient matrix, $[K]$, is decomposed into the multiplication of three matrices, as follows:

$$[K] = [L][D][L^T], \tag{27}$$

where $[L]$ and $[D]$ are lower triangular and diagonal matrices, respectively. The update procedure to determine the generalized incremental displacement vector, $\Delta\overline{U}$ (Equation 26), is based on the full Newton method. In this method, tangent stiffness matrix, $[K]$, and residual vector, $\overline{R}$, are modified at each step and iteration. An error function, defined as $\Delta\overline{U}^T\overline{R}$ (residual work), is used to check the convergence against a prescribed tolerance. Also, the buckling load is calculated by controlling the determinant sign of $[K](\det[K] = \prod_i D_{ii})$.

NON-LINEAR ANALYSIS (SMEARED MODEL)

Shell rigidities are modified based on material properties, cross-sectional dimensions and spacing of stringers. The stringer-stiffened shell rigidities, according to Figure 3 and [9], are:

$$[A] = \begin{bmatrix} A_{11} & A_{12} & 0 \\ A_{12} & A_{22} & 0 \\ 0 & 0 & A_{66} \end{bmatrix} + \begin{bmatrix} E_1A_1/b_1 & 0 & 0 \\ 0 & 0 & 0 \\ 0 & 0 & 0 \end{bmatrix},$$

$$[B] = \begin{bmatrix} B_{11} & B_{12} & 0 \\ B_{12} & B_{22} & 0 \\ 0 & 0 & B_{66} \end{bmatrix} + \begin{bmatrix} E_1A_1e_1/b_1 & 0 & 0 \\ 0 & 0 & 0 \\ 0 & 0 & 0 \end{bmatrix},$$

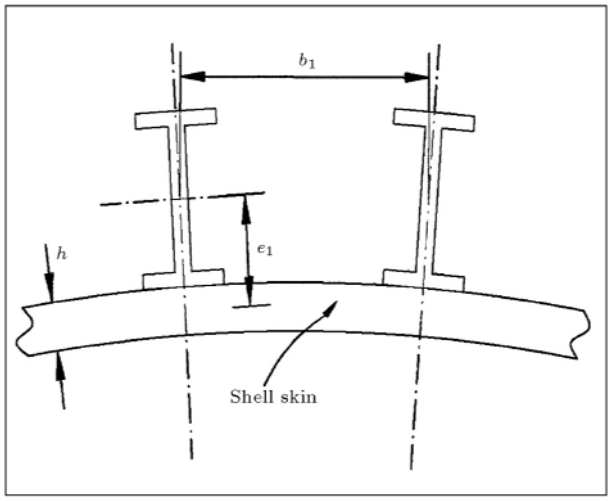

Figure 3. Geometry of a stringer-stiffened cylindrical shell.

$$[D] = \begin{bmatrix} D_{11} & D_{12} & 0 \\ D_{12} & D_{22} & 0 \\ 0 & 0 & D_{66} \end{bmatrix}$$

$$+ \begin{bmatrix} E_1(I_1 + A_1e_1^2)/b_1 & 0 & 0 \\ 0 & 0 & 0 \\ 0 & 0 & (G_1J_1/b_1)/4 \end{bmatrix}, \tag{28}$$

where E_1A_1 and G_1J_1 are the extensional and torsional rigidities of the stringer in the longitudinal direction, respectively, I_1 is the moment of inertia of the beam stiffener cross-section about its centroidal axis and e_1 is the stringer eccentricities (positive outside). The analysis continues as that of an un-stiffened shell, so, by eliminating δW_s^{int} and δW_λ from Equation 25, one has:

$$\delta W_{sh}^{\text{int}} \quad \delta W_{sh}^{\text{ext}} = 0. \tag{29}$$

NUMERICAL RESULTS AND DISCUSSIONS

The described analysis is used as a base for the development of a computer program. In the literature, most of the experimental and analytical results of stringer-stiffened shells buckling load are restricted to those of an isotropic material and a smeared stiffener approach. The first numerical example, which serves as verification for the current analysis, including several isotropic outside stringer-stiffened cylinders under axial compression, external pressure and a combination of both [1,7,10,20], are analyzed by the current discrete and smeared geometrical non-linear methods. Another numerical study is designed to compare the results of miscellaneous stringer-stiffened cylindrical shells, different in shell lay-ups, stiffener geometry, stringer spacing and method of analysis (discrete vs. smeared). The results are presented in the form of interaction buckling curves.

Table 1. Outside stringer-stiffened cylindrical shells dimensions ($E = 7500$ kg/mm^2, $\nu = 0.3$).

Case	L (mm)	R (mm)	h (mm)	n_s	(A_1/b_1h)	(e_1/h)	(I_1/bh^3)	(G_1J_1/bD)
A	78.618	120.56	0.204	56	0.717	3.670	2.400	19.839
B	965.20	242.57	0.719	60	1.028	5.830	9.629	16.912
C	200.00	120.27	0.249	84	0.666	4.030	2.770	7.505
D	130.00	120.10	0.254	85	0.590	3.420	1.680	6.563

Table 2. Comparison of experimental and analytical buckling load for various stringer-stiffened cylindrical shells.

Case	Type of Loading	Experimental Results (m, n_{cr})	Geometrical Non-Linear Analysis	
			Smeared Model (M, n_{cr})	Discrete Model (M, n_{cr}, N)[a]
A	Axial comp. (kg/mm)	4.356 [1] ——	6.110 (10,12)	4.250 (10,11,10)
B	Axial comp. (kg/mm)	20.43 [20][b] (1,6)	20.39 (10,6)	21.45 (10,5,13)
***C*1**	External press. (kg/mm^2)	0.001355 [7] (1,10)	0.001316 (10,11)	0.001480 (10,11,10)
***C*2**	Comb. press. (kg/mm^2)	0.001110 [7][c] (1,9)	0.001095 (10,11)	0.001270 (10,10,10)
D	Axial comp. (kg/mm)	5.334 [10] (1,9)	5.370 (10,11)	5.450 (10,10,10)

a: M and N represent number of non-zero terms in the axial and circumferential direction, respectively.

b: This result is related to smeared linear theory.

c: q_{cr} in the presence of constant axial compression ($P = 1.0587$ kg/mm).

ISOTROPIC STIFFENED CYLINDERS

Shell and stringer geometries of four isotropic outside stringer-stiffened cylindrical shells with a various number of stringers are shown in Table 1. For all specimens, $E = 7500$ kg/mm^2, $\nu = 0.3$ and boundary conditions are classical simply supported. Experimental results for different loading types, along with the current analysis buckling loads and their corresponding modes, are indicated in Table 2. Due to using several terms to approximate displacements and rotations in the circumference, discrete model buckling load predictions are in good agreement with those of experimental results. Although, in cases B, C and D, differences in the results of discrete and smeared geometrical nonlinear analyses are negligible, in case A, the variation is significant. In this case, A, local effect (panel instability) is the dominant factor in discrepancy between the results of smeared analysis and those of discrete analysis and experiment.

INTERACTION BUCKLING CURVES

Extensive studies exploring the effects of stringer discreteness, shell stacking sequences and location of stiffener (inside vs. outside) on interaction buckling curves are carried out. According to Figure 1, the dimensions of the assumed shell are; $R = 100$ mm, $L = 100$ mm and $h = 1$ mm. Also, referring to Figure 3, for stiffeners, $A_1/b_1h = 0.232$, $e_1 = 3.0$ mm (outside) and $e_1 = -3.0$ mm (inside). In all cases, the stringer height is constant but its width varies. Shell and stiffener material properties are $E_{11} = 140$ KN/mm^2, $E_{22} = 9.1$ KN/mm^2, $G_{12} = 4.3$ KN/mm^2, $G_{13} = 4.7$ KN/mm^2, $G_{23} = 5.9$ KN/mm^2 and $\nu_{12} = 0.3$. Stringer lay-up is taken as constant, (0), and shell stacking sequences vary according to the following arrangements: $(0)_8$, $(90)_8$, $(0/90/0/90)_s$, $(45/-45)_{4T}$, $(75/-75)_{4T}$.

Figure 4 illustrates the convergence of an axial buckling load versus an increase in number of stringers in the circumference for the above mentioned shell architecture of outside stringer-stiffened composite shells. Axial critical loads for un-stiffened shells are also indicated in this figure. For all shell lay-ups except $(0)_8$, despite differences in buckling loads, the trends of convergence are similar and local instability in the case of 50 stringers becomes negligible. In the case of shell arrangement $(0)_8$, due to lack of stiffening in the circumferential direction, even for 50 stringers or more, panel instability plays a fundamental role in the

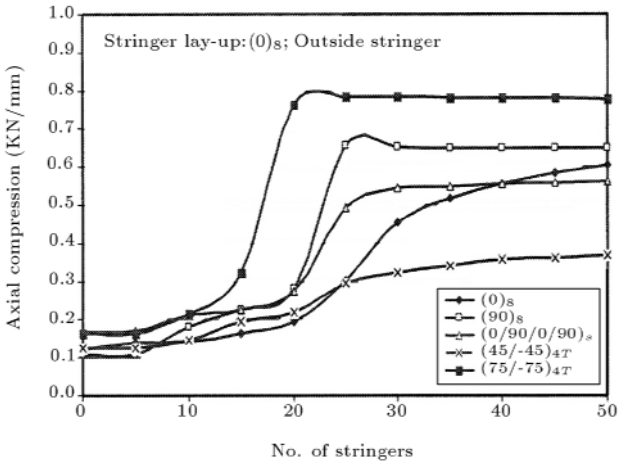

Figure 4. Convergence of axial buckling compression of various stringer-stiffened cylinders with increasing number of stringers.

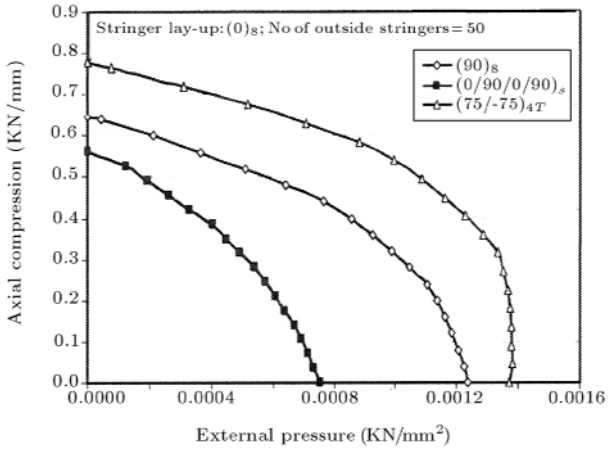

Figure 6. Effect of various shell lay-ups on interaction buckling curve of outside stringer-stiffened cylinder (discrete model).

overall buckling load. It is also observed, with respect to Figure 4, that there is a considerable change in the load carrying capacity of stiffened shells when the number of stringers increases from 10 to 30. Figure 5 shows interaction buckling curves derived based on a smeared stiffener approach for various outside stringer-stiffened cylinders. Stiffened shells with an anti-symmetric lay-up, $(75/\ \ 75)_{4T}$, exhibit a more stable area. Similar curves, according to discrete analysis for inside and outside stringer-stiffened shells, are plotted in Figures 6 and 7. Again, shell lay-up, $(75/\ \ 75)_{4T}$, is suitable for outside stiffening but, in an inside case, this preference mainly belongs to a $(0/90/0/90)_s$ arrangement. Figures 8 to 10 dictate that for all shell lay-ups and both discrete and smeared analysis, outside stiffening produces substantially more strength to buckling than that of an inside one. Figures 11 to 13, indicate influences of stringer discreteness with a change in the number of stringers, along with a

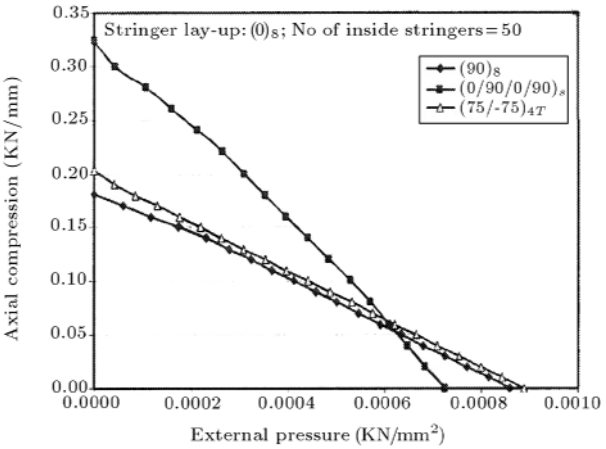

Figure 7. Effect of various shell lay-ups on interaction buckling curve of inside stringer-stiffened cylinder (discrete model).

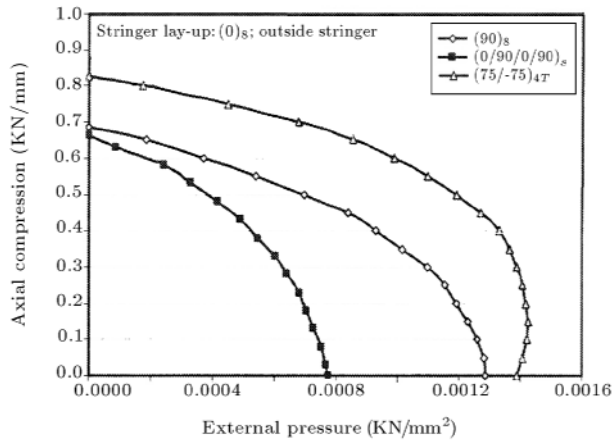

Figure 5. Comparison of different outside stringer-stiffened composite cylindrical shells for interaction buckling curve (smeared model).

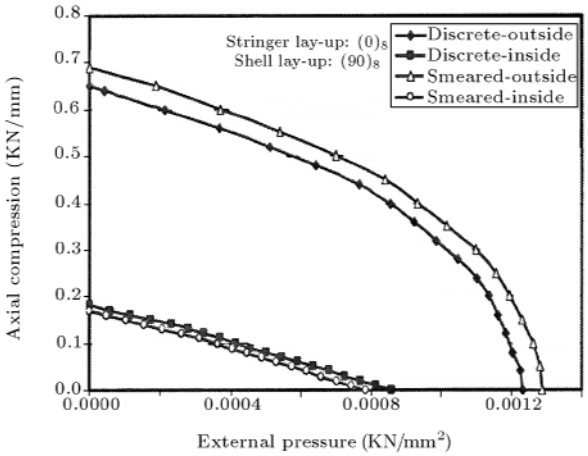

Figure 8. Effect of stringer location (inside vs. outside) and stringer modeling (smeared vs. discrete) on interaction buckling curve of stiffened shells (shell lay-up: $(90)_8$).

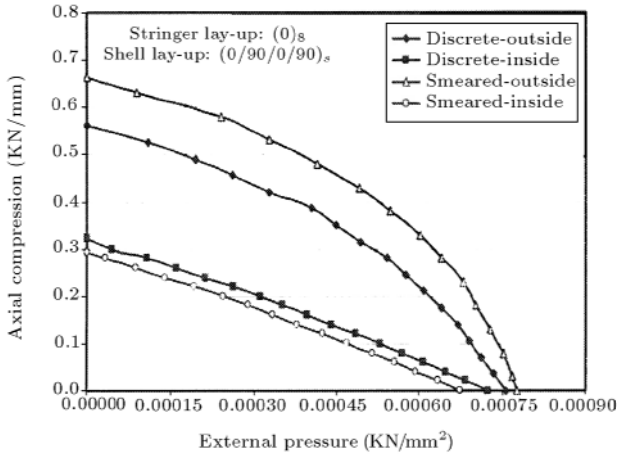

Figure 9. Effect of stringer location (inside vs. outside) and stringer modeling (smeared vs. discrete) on interaction buckling curve of stiffened shells (shell lay-up: $(0/90/0/90)_s$).

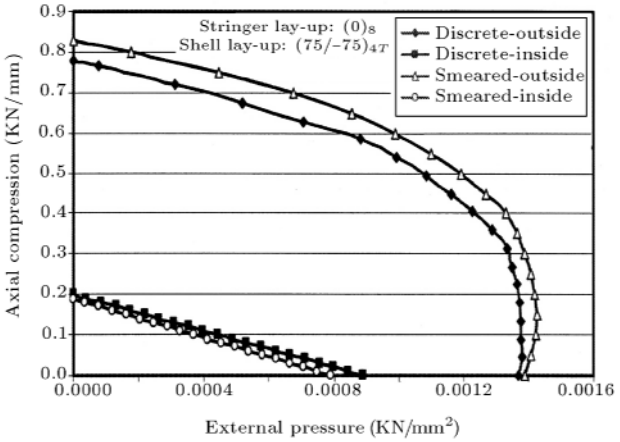

Figure 10. Effect of stringer location (inside vs. outside) and stringer modeling (smeared vs. discrete) on interaction buckling curve of stiffened shells (shell lay-up: $(75/\quad 75)_{4T}$).

variation of shell architecture for outside stringer-stiffened shells. Variation of the interaction buckling curve for a 10-stringer case, relative to the other two cases (30 and 50) is noticeable. Figure 11 shows some increase in the external pressure buckling strength in the presence of low axial compression ($P/P_{cr} < 0.3$). This effect can be explained by considering two factors; first, axial load eccentricity, which produces initial positive circumferential strain, ε_θ (axial compression is applied through the shell middle surface) and, second, the large ratio of A_{22}/A_{12} in the case of shell lay-up $(90)_8$. These parameters affect the circumferential force, $N_\theta (N_\theta = A_{12}\varepsilon_x + A_{22}\varepsilon_\theta)$, which, in turn, releases some compression force produced by applied external pressure. For other shell arrangements, despite existing load eccentricity, the stiffness ratio, A_{22}/A_{12}, is not so high to substantially reduce circumferential compres-

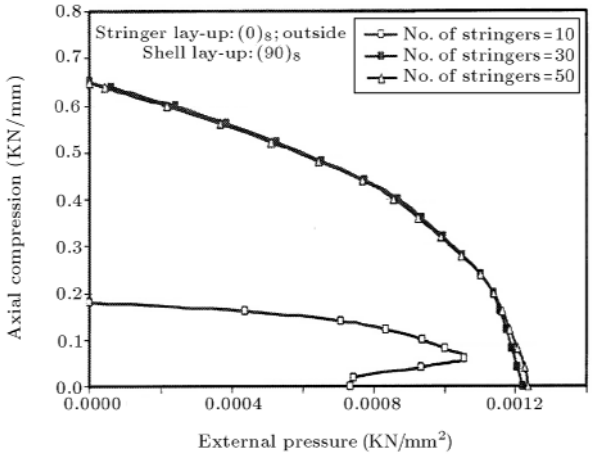

Figure 11. Influence of number of stringers on the interaction buckling curve of discretely stringer-stiffened cylindrical shells (shell lay-up: $(90)_8$).

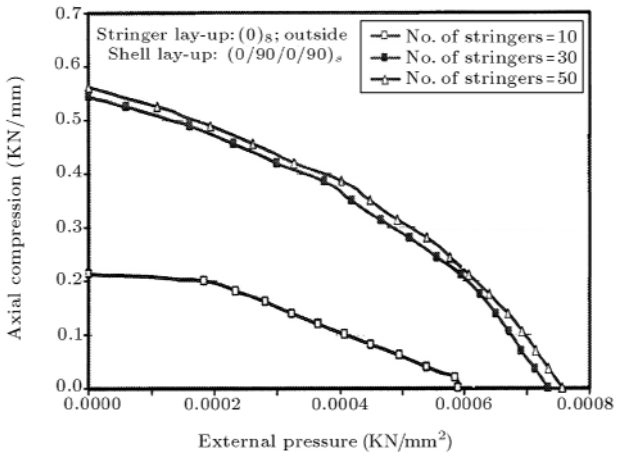

Figure 12. Influence of number of stringers on the interaction buckling curve of discretely stringer- stiffened cylindrical shells (shell lay-up: $(0/90/0/90)_s$).

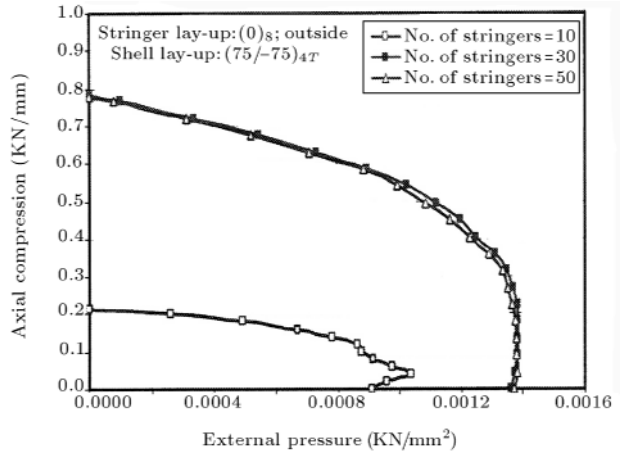

Figure 13. Influence of number of stringers on the interaction buckling curve of discretely stringer-stiffened cylindrical shells (shell lay-up: $(75/\quad 75)_{4T}$).

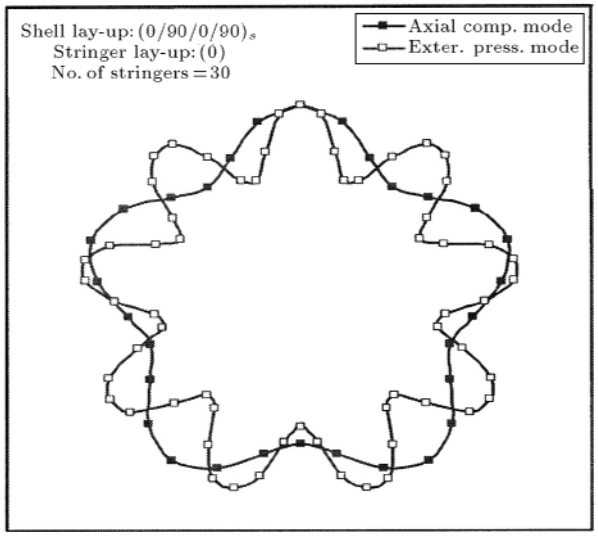

Figure 14. The variation limits of outside stringer-stiffened shell circumferential buckling mode for shell lay-up $(0/90/0/90)_s$.

sion. Also, with an increase in the number of stiffeners ($N_{str.} \geq 30$) and a dominating global buckling mode, buckling strength to combined loading noticeably increases and the mentioned effect decreases.

Variation of the circumferential wave number, n_{cr}, is equivalent to the change, in a tangent direction, of the interaction buckling curve and, consequently, the more alteration of n_{cr}, the more non-linearity of the buckling curve. Figure 14 indicates the lower and upper bounds of the circumferential mode for outside stiffening with shell lay-up $(0/90/0/90)_s$ whose wave number varies from $n_{cr} = 5$ (axial compression buckling mode) to $n_{cr} = 9$ (external pressure buckling mode). These limits for shell arrangements $(90)_8$ and $(75/\ \ 75)_{4T}$ are (5,8) and (6,9), respectively. For inside stiffening, these numbers are restricted to $n_{cr} = 6$ for shell lay-up $(75/\ \ 75)_{4T}$, $n_{cr} = 5, 6$ in the case of shell lay-up $(90)_8$ and $n_{cr} = 7, 8$ for symmetric cross-ply arrangement, $(0/90/0/90)_s$ (Figures 8 to 10).

CONCLUSIONS

Discrete and smeared as two approaches in geometrical non-linear analyses have been implemented to study isotropic and orthotropic equally spaced stringer-stiffened cylindrical shells subject to combined axial compression and external pressure. On the basis of the case studies, the following conclusions may be drawn:

1. For isotropic outside stringer-stiffened cylinders, the discrete model predicts the axial buckling load more accurately than those of external and combined pressures and the maximum deviation from an experimental axial buckling load is less than 5 percent. Also, in all loading cases, the circumferential wave number, n_{cr}, obtained, based on smeared model analysis, is greater than that of a discrete one;
2. For outside stringer-stiffened composite cylindrical shells, shell stacking sequence $(75/\ \ 75)_{4T}$ encloses a more stable area, while shell lay-up $(0/90/0/90)_s$ exhibits less stability against combined axial compression and external pressure. In inside stiffening cases, arrangement $(0/90/0/90)_s$ encircles a greater stable zone than those of lay-ups $(90)_8$ and $(75/\ \ 75)_{4T}$;
3. For all shell stacking sequences and both models of stringer (smeared vs. discrete), outside stiffening shows more stability against combined loading than that of inside stiffening, especially at a high ratio of axial compression to external pressure. Also, due to a wide range of mode variation, outside stringer-stiffened cylinders involve a non-linear form, while inside-stiffened shells take a nearly linear appearance;
4. Apart from shell stacking sequences, in outside stiffening cases, interaction buckling curves obtained, based on a smeared model analysis, encompass those curves plotted according to a discrete model analysis. The trend for the inside stiffening case is opposite;
5. In the case of outside stiffening, the number of stringers in the circumference play a fundamental role in estimating critical load and the interacting buckling curve. For 10 stringers, panel instability (shell skin buckling between stiffeners) considerably affects buckling load, while, in the cases of 30 and 50 stringers, local effects diminish and the contribution of stiffeners in the buckling response increases.

REFERENCES

1. Weller, T. and Singer, J. "Experimental studies on the buckling under axial compression integrally stringer-stiffened circular cylindrical shells", *Journal of Applied Mechanics*, **44**(4), pp 721-730 (1977).
2. Singer, J. and Abramovich, H. "Vibration techniques for definition of practical boundary conditions in stiffened shells", *AIAA Journal*, **17**(7), pp 762-769 (1979).
3. Weller, T. "Combined stiffening and in-plane boundary conditions effects on the buckling of circular cylindrical stiffened shells", *Comput. & Struct.*, **9**(1), pp 1-16(1978).
4. Sheinman, I., Shaw, D. and Simitses, G.J. "Nonlinear analysis of axially loaded laminated cylindrical shells", *Comput. & Struct.*, **16**, pp 131-137 (1983).
5. Bushnell, D. "PANDA- interactive program for minimum weight design of stiffened cylindrical panels and shells", *Comput. & Struct.*, **16**, pp 167-185 (1983).
6. Wang, J.T.S. and Hsu, T.M. "Discrete analysis of stiffened composite cylindrical shells", *AIAA Journal*, **23**(11), pp 1753-1761 (1985).

7. Abramovich, H., Weller, T. and Singer, J. "Effect of sequence of combined loading on buckling of stiffened shells", *Experimental Mechanics*, **28**(1), pp 1-13 (1988).
8. Ji, Z.Y. and Yeh, K.Y. "General solution for nonlinear buckling of nonhomogeneous axial symmetric ring- and stringer-stiffened cylindrical shells", *Comput. & Struct.*, **34**(4), pp 585-591 (1990).
9. Shen, H.S. "Post-buckling analysis of imperfect stiffened laminated cylindrical shells under combined external pressure and axial compression", *Comput. & Struct.*, **63**(2), pp 335-348 (1997).
10. Shen, H.S., Zhou, P. and Chen, T.Y. "Postbuckling analysis of stiffened cylindrical shells under combined external pressure and axial compression", *Thin-Walled Structures*, **15**, pp 43-63 (1993)
11. Dawe, D.J. and Wang, S. "Postbuckling analysis of composite laminated panels", *AIAA Journal*, **38**(11), pp 2160-2170 (2000)
12. Spagnoli, A. "Different buckling modes in axially stiffened conical shells", *Engineering Structures*, **23**, pp 957-965 (2001).
13. Haixu, D. "Strength and stability of double cylindrical shell structure subjected to hydrostatic external pressure-II: Stability", *Marine Structures*, **16**(5), pp 397-415 (2003).
14. Yaffe, R. and Abramovich, H. "Dynamic buckling of cylindrical stringer stiffened shells", *Comput. & Struct.*, **81**(8-11), pp 1031-1039 (2003).
15. Bonet, J. and Wood, R.D., *Nonlinear Continuum Mechanics for Finite Element Analysis*, Cambridge University Press, Cambridge, UK (1997).
16. Rastogi, N. "Load transfer in the stiffener-to-skin joints of a pressurized fuselage", Doctoral Dissertation, Department of Aerospace and Ocean Engineering, Virginia Polytechnic Institute and State University, Blacksburg, Virginia, USA (1995).
17. Jones, R.M., *Mechanics of Composite Material*, Hemisphere, Washington D.C., USA (1975).
18. Woodson, M.B. "Optimal design of composite fuselage frames for crashworthiness", Doctoral Dissertation, Department of Aerospace and Ocean Engineering, Virginia Polytechnic Institute and State University. Blacksburg, Virginia, USA (1994).
19. Schweizerhof, K. and Ramm, E. "Displacement dependent pressure load in nonlinear finite element analysis", *Comput. & Struct.*, **18**(6), pp 1099-1114 (1984).
20. Brush, D.O. and Almorth, B.O., *Buckling of Bars, Plates, and Shells*, McGraw-Hill, New York, USA (1975).